EAI Endorsed Transactions
on Industrial Networks and Intelligent Systems
Research Article EAI.EU

Exact Outage Analysis of Cognitive Energy Harvesting Relaying Networks under Physical Layer Security

Sang Quang Nguyen[1,*], Huy T. Nguyen[2], Dong Doan Van[3], Won-Joo Hwang[2]

[1]Institute of Fundamental and Applied Sciences, Duy Tan University, Ho Chi Minh City 700000, Vietnam
[2]Department of Information and Communication System, Inje University, 197, Gimhae, Gyeongnam, Korea
[3]Faculty Electrical and Electronic Engineering, Ho Chi Minh City University of Transport, Ho Chi Minh City 700000, Vietnam

Abstract

In this paper, we study the secure communication of cognitive energy harvesting relay networks when there exist multiple eavesdroppers who can overhear the message of the second hop, and multiple primary users are present. The data transmission from the secondary source to the secondary destination is assisted by the best decode-and-forward relay, which is selected by means of three relay selection schemes. We study the system security performance by deriving the exact analytical secrecy outage probability. These analytical expressions are then verified by comparison to the results of Monte Carlo simulations. Herein we evaluate and discuss the outage performance of the three schemes under variations in important system parameters: the number and locations of relay nodes, primary user nodes, and eavesdroppers; the transmit power threshold; the energy harvesting efficiency coefficient; the power splitting ratio; and the target secure rate.

Keywords: Energy harvesting; Cognitive radio; Cooperative communication; Physical layer security; Relay selection; Power splitting; Decode-and-forward
Received on 14 December 2018, accepted on 17 December 2018, published on 28 March 2019

doi:10.4108/eai.28-3-2019.157119

*Corresponding author. Email: nguyenquangsang3@dtu.edu.vn

1. Introduction

Recently, the simultaneous wireless information and power transfer (SWIPT) technique has attracted more and more attention in wireless networks as an efficient solution to prolong the lifetime of energy-constrained wireless devices. An ideal SWIPT was first proposed for the scenario in which the receiver can simultaneously harvest energy and detect information from the same received signal [1]. Subsequently, practical energy harvesting receiver designs for SWIPT were proposed and studied, based on two architectures: power-splitting (PS) and time switching (TS) [2, 9, 10, 12, 22]. In such designs, the signal received at the PS receiver is split into two parts, one for harvesting the energy

and the other one for decoding the information; this splitting is carried out in accordance with a power splitting ratio. Within a time block, the TS receiver harvests energy from the received radio-frequency signal during an initial interval and then switches to decoding the information during the remaining interval.

As a means to combat multipath fading in wireless communication, cooperative communication is an effective solution that increases the diversity capacity [3, 4]. Decode-and-forward (DF) and amplify-and-forward (AF) are the two main strategies applied at relay nodes in cooperative networks. In DF mode, the relay node detects information from the received signal and then re-encodes and forwards it in the next hop. In AF mode, the relay only amplifies the received signal and forwards it; this is simpler than DF, but has the drawback that the noise within the received signal is also amplified. Some performance metrics as outage probability, average sum-rate, and average symbol error rate for the semi-blind (partial channel state information) have been analyzed for the conditions of Rayleigh fading channels [5], the Nakagami-m fading environment [6], and the generalized-K fading channel [7]. A hybrid AF-DF protocol has been considered for multihop relaying networks [8]. Several works have addressed the application of energy harvesting techniques in energy-constrained relay nodes of cooperative systems. In [9], the authors design three wireless power transfer policies and analyzed their throughput in two-way relaying networks in which the TS architecture was employed at an energy-constrained AF relay node. In [10], the authors derive expressions of the throughput, outage probability, and ergodic capacity for a dual-hop relaying system, considering the use of both TS and PS architectures at an AF relay node. Other works have addressed the case of multiple sourceâĂŞdestination pairs communicating with each other via a DF energy harvesting relay [11, 12]. In [11], the authors focus on the distribution of harvested energy among the multiple users and their impact on the system performance in a TS architecture. In [12], the authors investigate the power allocation based on maximizing the total rate for a PS architecture. Optimal power and time fraction allocation, and optimal power allocation with a fixed time fraction have both been proposed to maximize the achievable average data rate in a DF energy harvesting relaying system [13]. In [14], the authors study the performance analysis of an energy harvesting relaying network using the help of multiple relay nodes. Unlike the fixed locations considered in previous works, in [15] the authors considered multiple randomly located DF energy harvesting relay nodes, for which the density function for the wireless channels is characterized by stochastic geometry.

Cognitive radio is regarded as an efficient technique to enhance the spectrum efficiency in wireless communication systems [16]. It allows secondary users (unlicensed users) to utilize the spectrum bands of primary users (licensed users) without interfering with primary usersâĂŹ communications. In the underlay mode of cognitive radio, secondary users transmit simultaneously with primary users over the same spectrum without degrading the quality of service of the primary transmission by keeping the interference to the primary users under a predefined threshold [17]. The outage performance of a dual-hop underlay cognitive radio network over the independent non-identically distributed Nakagami-m fading channel is studied in [17]. In [18], the authors extended [17] considering the best relay selection strategy in a cognitive relaying network with the presence of multiple AF relay nodes. An algorithm has been proposed to maximize the throughput in a cognitive AF [19] or DF [20] relaying network in which energy harvesting based on PS is applied at the relay. In another work, the PS and TS architectures were utilized at the best relay in an underlay cognitive DF relaying network [21]. The impact of transceiver hardware impairments upon the outage performance and throughput of a DF two-way energy harvesting relaying network is considered in [22].

Due to the broadcast nature of the wireless medium, information can be overheard and extracted by unwanted eavesdroppers. Physical layer security (PLS) has received considerable attention from researchers as a means to solve this issue. Wyner first defined the achievable secrecy rate (ASR) as the maximum rate of reliable information sent from the source to its destination in the presence of eavesdroppers [23]. Wyner showed that the communication between source and destination is secure when the ASR is larger than the required secrecy rate. Following this finding, PLS has been considered in Gaussian wiretap channels [24], and has been extended to broadcast channels [25] as well as to fading channels [26]. Considering the PLS in CRN has attracted attention from various researchers [27–30]. In [27] the authors studied the security of CRN with the presence of a multiple-antennas eavesdropper. Several relay selection strategies to choose two relays for secure communication in cognitive DF relay networks [28], i.e., the one relay help the source forward information to destination, the other relay confound the eavesdropper by transmitting the jamming signal. A secure switch-and-stay combining protocol is studied in CRN to overcome the limitation of the continuous requirement the channels state information at all relays [29]. Secure communication of the AF and DF energy harvesting relaying networks under wiretapping by an eavesdropper has also been studied [30]. The issue of eavesdropper's ability to collaborate, to exchange the

information obtained from the source and relays, has been studied in [32].

To the best of our knowledge, there has been now study on the jointly energy harvesting technique in cognitive radio networks and under wiretapping of eavesdroppers. This motivates us to analyze the exact secrecy outage probability of the secure communication of the underlay cognitive relaying networks. In this model, we consider the communication between a secondary source and secondary destination based on the assist of multiple intermediate secondary relays under the presence of multiple primary users and eavesdroppers. For the performance evaluation and comparison, the exact expressions of the secrecy outage probability for three partial relay selection schemes are derived. Three relay selection schemes for choosing the one best relay, which harvests and decode the information from the received signal and forward to the destination, are presented as: 1) the maximum channel gain from the source to the relays, called the MaSR scheme, 2) the MiRP scheme stand for minimum channel gain from the relays to the primary users, 3) the minimum channel gain from the relays to the eavesdroppers, MiRE. The Monte Carlo simulations are used to verify our theoretical analysis.

The rest of the paper is organized as follows. Section 2 presents the system model and formulas expressing the three relay selection schemes. Section 3 presents the transmission operation of the system in which the energy harvesting-based power splitting architecture is applied at the selected relay. Section 4 presents secrecy outage probability analyses for the three schemes studied. Section 5 presents system performance with high Q/N_0. Section 6 presents numerical results from the simulations and theoretical analyses. Finally, Section 7 presents our conclusions.

Notation: The notation $\mathcal{CN}(a,b)$ denotes a circularly symmetric complex Gaussian random variable (RV) with mean a and variance b. $\mathcal{E}\{.\}$ denotes mathematical expectation. The functions $f_X(.)$ and $F_X(.)$ present the probability density function (PDF) and cumulative distribution function (CDF) of RV X. The function $\Gamma(x,y)$ is an incomplete Gamma function [31, Eq. 8.350.2]. $C_b^a = \frac{b!}{a!(b-a)!}$. Pr[.] returns the probability. $[x]^+$ returns x if $x \geq 0$ and 0 if $x < 0$.

2. System model

As shown in Figure 1, we consider a system model of an underlay cooperative cognitive network under physical layer security. The secondary network consists a source node (S), a destination node (D), M energy-constrained relays (R_m, $m \in \{1,2,...,M\}$) in cluster R, and L eavesdroppers (E_l, $l \in \{1,2,...,L\}$) in cluster E; also, there are N primary receivers (P_n, $n \in \{1,2,...,N\}$) in cluster P, located in the primary network. We note that the primary transmitters (not shown in Fig. 1) are located far enough from the secondary network that their interference to the secondary nodes can be ignored [21]. Each node is equipped with a single antenna operating in half-duplex mode.

In Figure 1, we denote $\left(h_{SR_m}, d_{SR_m}\right)$, $\left(h_{SP_n}, d_{SP_n}\right)$, $\left(h_{R_mD}, d_{R_mD}\right)$, $\left(h_{R_mP_n}, d_{R_mP_n}\right)$ and $\left(h_{R_mE_l}, d_{R_mE_l}\right)$ as the Rayleigh fading channel coefficients and distances of the links $S-R_m$, $S-P_n$, R_m-D, R_m-P_n, and R_m-E_l, respectively, where P_n, R_m, and E_l denote the nth primary receiver in cluster P, the mth relay in cluster R, and the lth eavesdropper in cluster E. Thus, the corresponding channel gains $g_\chi = \left|h_\chi\right|^2$, with $\chi \in \{SR_m, SP_n, R_mD, R_mP_n, R_mE_l\}$, are exponentially distributed independent random variables (RVs) with parameters $\lambda_\chi = \left(d_\chi\right)^\beta$, where β denotes the path loss exponent. We obtain the corresponding cumulative distribution functions (CDF) and probability density functions (PDF) of the RVs g_χ as $F_{g_\chi}(x) = \lambda_\chi e^{-\lambda_\chi x}$ and $f_{g_\chi}(x) = 1 - e^{-\lambda_\chi x}$, respectively. The distances between the two nodes in a cluster are insignificant compared to the distances between nodes not within the same cluster [30]. Hence, we can denote $d_{SR_m} \triangleq d_{SR}$, $d_{SP_n} \triangleq d_{SP}$, $d_{R_mD} \triangleq d_{RD}$, $d_{R_mP_n} \triangleq d_{RP}$, and $d_{R_mE_l} \triangleq d_{RE}$, with $m \in \{1,2,...,M\}$, $n \in \{1,2,...,N\}$, $l \in \{1,2,...,L\}$; the parameters then can be denoted as $\lambda_{SR_m} \triangleq \lambda_{SR}$, $\lambda_{SP_n} \triangleq \lambda_{SP}$, $\lambda_{R_mD} \triangleq \lambda_{RD}$, $\lambda_{R_mP_n} \triangleq \lambda_{RP}$, and $\lambda_{R_mE_l} \triangleq \lambda_{RE}$. We assume that no direct links exist between S and D nor between S and cluster E due to deep shadowing [30], and that cluster E is located near D to allow eavesdropping on D [30]. After the set up phase, the destination has perfect channel coefficients for all links [30]; then, D selects a best relay R_b from the M available nodes to receive and harvest the energy from the RF signal, which is transmitted from S in the first hop and then decoded and forwarded to D under eavesdropping by L eavesdroppers in the second hop.

Three partial relay selection schemes are considered throughout this paper to increase the system performance as well as to reduce the power consumption of the source node. First, the relay R_b is selected by maximizing the channel gain of the $S-R_m$ link (called the MaSR strategy) to increase the amount of harvested energy and the decoding performance at the relay. Second, to reduce the interference from the selected relay to all of the N primary receivers, the relay R_b is chosen from the M available nodes that minimizes the channel gain of the R_m-P_n link (called the MiRP strategy). Third, R_b is selected by minimizing the channel gain of the R_m-E_l link (called the MiRE strategy). These three relay selection schemes are formulated respectively as

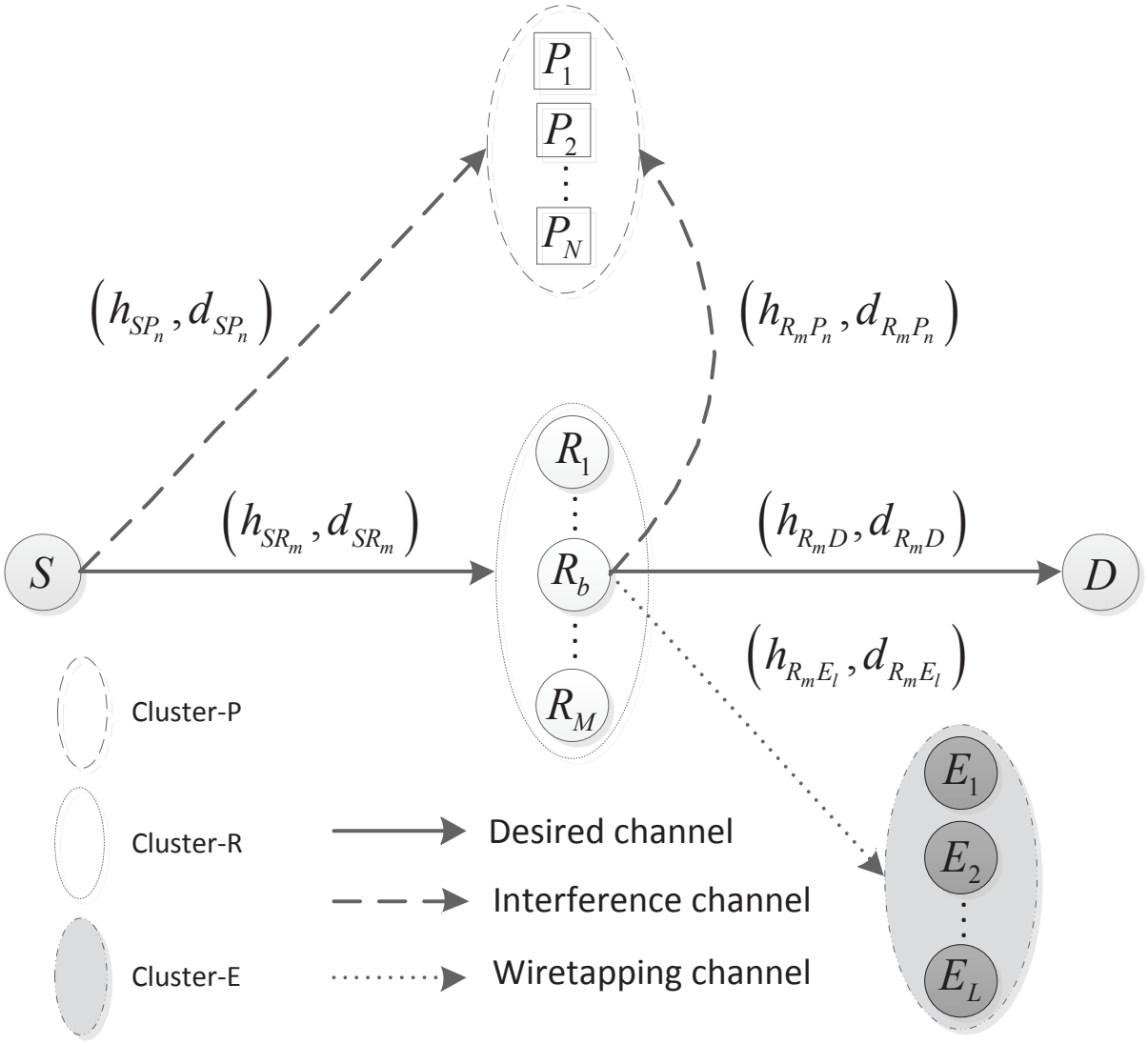

Figure 1. System model

follows.

$$R_b = \arg \max_{m=1,2,\ldots,M} g_{SR_m} \tag{1}$$

$$R_b = \arg \min_{m=1,2,\ldots,M} \left(\max_{n=1,2,\ldots,N} g_{R_mP_n} \right) \tag{2}$$

$$R_b = \arg \min_{m=1,2,\ldots,M} \left(\max_{l=1,2,\ldots,L} g_{R_mE_l} \right) \tag{3}$$

3. Energy harvesting-based power splitting and transmission operation

In this section, we consider energy harvesting based on the power splitting protocol, with the power splitting ratio of $\rho \in (0,1)$ for energy harvesting and $(1-\rho)$ for decoding the source information at the best relay R_b in the first time slot (i.e., the first time interval: $T/2$) [10, Fig. 3]. The received signals for energy harvesting and for information decoding at R_b are given respectively by

$$y_{SR_b,eh}(t) = \sqrt{\rho P_S} h_{SR_b} x(t) + \sqrt{\rho} n_{SR_b}(t) \tag{4}$$

$$y_{SR_b,id}(t) = \sqrt{(1-\rho) P_S} h_{SR_b} x(t) + \sqrt{(1-\rho)} n_{SR_b}(t), \tag{5}$$

where $P_S = \frac{Q}{\max\limits_{n=1,2,\ldots,N} g_{SP_n}}$ is the adapted transmit power of the source S, with Q being the interference threshold for the primary receivers [27]; $x(t)$ is the transmitted

signal, with $\mathcal{E}\left\{|x(t)|^2\right\}=1$; and $n_{SR_b}(t)\sim CN(0,N_0)$ denotes the additive white Gaussian noise (AWGN) at R_b.

From (4), we obtain the following expression for the energy harvested at R_b during time $T/2$:

$$E_{SR_b}=\eta\rho P_S g_{SR_b}(T/2), \tag{6}$$

where $0\le\eta\le1$ is the harvesting efficiency coefficient, which depends on the rectification process and the energy harvesting circuitry [19]. The harvested noise energy is ignored because it is insignificant compared to the overall harvested energy [19]. The RF signal expressed by (5) is downconverted to a baseband signal [10]; this baseband signal as sampled at R_b can be expressed as

$$y_{SR_b,id}(k)=\sqrt{(1-\rho)P_S}h_{SR_b}x(k)+\sqrt{(1-\rho)}n_{SR_b}(k)+n^c_{SR_b}(k) \tag{7}$$

where $n^c_{SR_b}(k)\sim CN(0,\mu N_0)$, with $\mu>0$, denotes the AWGN at the converting unit.

The relay R_b decodes the information and then re-encodes it for forwarding to the destination D under eavesdropping by L eavesdroppers. The transmit power at R_b is adapted, in order not to exceed the threshold Q, as $P_{Rb}=\min\left(\frac{E_{SR_b}}{T/2},\frac{Q}{\max\limits_{n=1,2,\dots,N}g_{R_bP_n}}\right)=\min\left(\frac{\eta\rho Q g_{SR_b}}{\max\limits_{n=1,2,\dots,N}g_{SP_n}},\frac{Q}{\max\limits_{n=1,2,\dots,N}g_{R_bP_n}}\right)$. The received sampled baseband signals at S and E_l can be expressed respectively as

$$y_{R_bD}(k)=\sqrt{P_{R_b}}h_{R_bD}x(k)+n_{R_bD}(k)+n^c_{R_bD}(k) \tag{8}$$

$$y_{R_bE_l}(k)=\sqrt{P_{R_b}}h_{R_bE_l}x(k)+n_{R_bE_l}(k)+n^c_{R_bE_l}(k), \tag{9}$$

where $n_{R_bD},n_{R_bE_l}(k)\sim CN(0,N_0)$ and $n^c_{R_bD}(k),n^c_{R_bE_l}\sim CN(0,\mu N_0)$.

The achievable secrecy rates for the first hop ψ_1 can be obtained from (7), and for the second hop ψ_2 can be obtained from (8) and (9) as follows:

$$\begin{aligned}\psi_1&=\left[\tfrac{1}{2}\log_2\left(1+\frac{(1-\rho)P_S}{(1-\rho+\mu)N_0}g_{SR_b}\right)\right]^+\\&=\left[\tfrac{1}{2}\log_2\left(1+\frac{\omega_1 g_{SR_b}}{\max\limits_{n=1,2,\dots,N}g_{SP_n}}\right)\right]^+\end{aligned} \tag{10}$$

$$\begin{aligned}\psi_2&=\left[\tfrac{1}{2}\log_2\left(\frac{1+\frac{P_{R_b}g_{R_bD}}{(1+\mu)N_0}}{1+\frac{P_{R_b}\max\limits_{l=1,2,\dots,L}g_{R_bE_l}}{(1+\mu)N_0}}\right)\right]^+\\&=\left[\tfrac{1}{2}\log_2\left(\frac{1+g_{R_bD}\min\left(\frac{\omega_2 g_{SR_b}}{\max\limits_{n=1,2,\dots,N}g_{SP_n}},\frac{\omega_3}{\max\limits_{n=1,2,\dots,N}g_{R_bP_n}}\right)}{1+\left(\max\limits_{l=1,2,\dots,L}g_{R_bE_l}\right)\min\left(\frac{\omega_2 g_{SR_b}}{\max\limits_{n=1,2,\dots,N}g_{SP_n}},\frac{\omega_3}{\max\limits_{n=1,2,\dots,N}g_{R_bP_n}}\right)}\right)\right]^+\end{aligned} \tag{11}$$

where $\omega_1\triangleq\frac{(1-\rho)Q}{(1-\rho+\mu)N_0}$, $\omega_2\triangleq\frac{\eta\rho Q}{(1+\mu)N_0}$, and $\omega_3\triangleq\frac{Q}{(1+\mu)N_0}$.

4. Secrecy outage probabilities of relay selection schemes

In this section we analyze the secrecy outage probability (SOP) of the three relay selection schemes mentioned in Section 2: MaSR, MiRP, and MiRE. None of these SOP derivations include the assumption of high SNR used in previous work [14]. The SOP is defined as the probability the achievable secrecy rate of the system, i.e., $\min(\psi_1,\psi_2)$, is below a desired threshold secrecy rate ψ_t

$$P_{out}=\Pr[\min(\psi_1,\psi_2)<\psi_t]=1-\Pr[\psi_1\ge\psi_t,\psi_2\ge\psi_t] \tag{12}$$

Substituting (10) and (11) into (12), we have

$$\begin{aligned}P_{out}&=1-\Pr\left[\begin{array}{l}\frac{1}{2}\log_2(1+\omega_1 g)\ge\psi_t,\\ \frac{1}{2}\log_2\left(\frac{1+g_{R_bD}\min\left(\frac{\omega_2 g_{SR_b}}{\max\limits_{n=1,2,\dots,N}g_{SP_n}},\frac{\omega_3}{\max\limits_{n=1,2,\dots,N}g_{R_bP_n}}\right)}{1+\left(\max\limits_{l=1,2,\dots,L}g_{R_bE_l}\right)\min\left(\frac{\omega_2 g_{SR_b}}{\max\limits_{n=1,2,\dots,N}g_{SP_n}},\frac{\omega_3}{\max\limits_{n=1,2,\dots,N}g_{R_bP_n}}\right)}\right)\ge\psi_t\end{array}\right]\\&=1-(\Pr 1+\Pr 2)\end{aligned} \tag{13}$$

where g is a new RV denoted as $g\triangleq\frac{g_{SR_b}}{\max\limits_{n=1,2,\dots,N}g_{SP_n}}$; denoting the terms $\Pr 1=\Pr\left[\begin{array}{l}\frac{1}{2}\log_2(1+\omega_1 g)\ge\psi_t,\frac{1}{2}\log_2\left(\frac{1+\omega_2 g_{R_bD}g}{1+\omega_2\left(\max\limits_{l=1,2,\dots,L}g_{R_bE_l}\right)g}\right)\ge\psi_t,\\ \omega_2 g<\frac{\omega_3}{\max\limits_{n=1,2,\dots,N}g_{R_bP_n}}\end{array}\right]$;

$\Pr 2=\Pr\left[\begin{array}{l}\frac{1}{2}\log_2(1+\omega_1 g)\ge\psi_t,\frac{1}{2}\log_2\left(\frac{1+\frac{\omega_3 g_{R_bD}}{\max\limits_{n=1,2,\dots,N}g_{R_bP_n}}}{\frac{\omega_3}{\max\limits_{l=1,2,\dots,L}g_{R_bE_l}}+\frac{\omega_3}{\max\limits_{n=1,2,\dots,N}g_{R_bP_n}}}\right)\ge\psi_t,\\ \omega_2 g\ge\frac{\omega_3}{\max\limits_{n=1,2,\dots,N}g_{R_bP_n}}\end{array}\right]$

The terms $\Pr 1$ and $\Pr 2$ can be expressed in the following multiple integral forms:

$$\begin{aligned}\Pr 1&=\Pr\left[g\ge\tfrac{\theta-1}{\omega_1},g_3\ge\tfrac{\theta-1}{\omega_2 g}+\theta g_2,g_1<\tfrac{\omega_3}{\omega_2 g}\right]\\&=\int_{\frac{\theta-1}{\omega_1}}^{\infty}f_g(x)\int_0^{\frac{\omega_3}{\omega_2 x}}f_{g_1}(x_1)\int_0^{\infty}f_{g_2}(x_2)\\&\quad\int_{\frac{\theta-1}{\omega_2 x}+\theta x_2}^{\infty}f_{g_3}(x_3)dx_3dx_2dx_1dx\end{aligned} \tag{14}$$

$$\begin{aligned}\Pr 2&=\Pr\left[g\ge\tfrac{\theta-1}{\omega_1},g_3\ge\tfrac{\theta-1}{\omega_3}g_1+\theta g_2,g_1\ge\tfrac{\omega_3}{\omega_2 g}\right]\\&=\int_{\frac{\theta-1}{\omega_1}}^{\infty}f_g(x)\int_{\frac{\omega_3}{\omega_2 x}}^{\infty}f_{g_1}(x_1)\int_0^{\infty}f_{g_2}(x_2)\\&\quad\int_{\frac{\theta-1}{\omega_3}x_1+\theta x_2}^{\infty}f_{g_3}(x_3)dx_3dx_2dx_1dx\end{aligned}, \tag{15}$$

where $\theta\triangleq 2^{2\psi_t}$, $g_1\triangleq\max\limits_{n=1,2,\dots,N}g_{R_bP_n}$, $g_2\triangleq\max\limits_{l=1,2,\dots,L}g_{R_bE_l}$, and $g_3\triangleq g_{R_bD}$.

The PDF of g_3 is $f_{g_3}(x_3)=\lambda_{RD}e^{-\lambda_{RD}x_3}$ for all three cases of relay selection schemes. And the PDFs of g, g_1, and g_2 can be changed depending on the relay selection schemes as three subsection follows.

4.1. Secrecy outage probability of MaSR

The PDF of g_1, g_2 can be obtained as the same way as in Eq. (A2) of **Appendix A** , and the PDF of g can be expressed as in Eq. (A5) of **Appendix A**, as follows.

$$f_{g_1}(x_1) = N\lambda_{RP}\sum_{k=0}^{N-1} C_{N-1}^{k}(-1)^k e^{-(1+k)\lambda_{RP}x_1} \tag{16}$$

$$f_{g_2}(x_2) = L\lambda_{RE}\sum_{l=0}^{L-1} C_{L-1}^{l}(-1)^l e^{-(1+l)\lambda_{RE}x_2} \tag{17}$$

$$f_g(x) = MN\lambda_{SP}\lambda_{SR}\sum_{m=0}^{M-1} C_{M-1}^{m}(-1)^m \sum_{n=0}^{N-1}\frac{C_{N-1}^{n}(-1)^n}{\left[(1+n)\lambda_{SP}+(1+m)\lambda_{SR}x\right]^2} \tag{18}$$

The term Pr 1 can be expressed as follows, including substitution of the PDFs of g, g_1, g_2 and g_3 into Eq. (14) and subsequent manipulations.

$$\begin{aligned}
\Pr 1 &= \int_{\frac{\theta-1}{\omega_1}}^{\infty} f_g(x)\int_0^{\frac{\omega_3}{\omega_2 x}} f_{g_1}(x_1)\int_0^{\infty} f_{g_2}(x_2)\\
&\int_{\frac{\theta-1}{\omega_2 x}+\theta x_2}^{\infty} f_{g_3}(x_3)dx_3dx_2dx_1dx\\
&= L\lambda_{RE}\sum_{l=0}^{L-1}\frac{C_{L-1}^{l}(-1)^l}{(1+l)\lambda_{RE}+\theta\lambda_{RD}}\int_{\frac{\theta-1}{\omega_1}}^{\infty} f_g(x)\,e^{-\frac{(\theta-1)\lambda_{RD}}{\omega_2 x}}\\
&\int_0^{\frac{\omega_3}{\omega_2 x}} N\lambda_{RP}\sum_{k=0}^{N-1} C_{N-1}^{k}(-1)^k e^{-(1+k)\lambda_{RP}x_1}dx_1dx\\
&= L\lambda_{RE}\sum_{l=0}^{L-1}\frac{C_{L-1}^{l}(-1)^l}{(1+l)\lambda_{RE}+\theta\lambda_{RD}}N\\
&\sum_{k=0}^{N-1}\frac{C_{N-1}^{k}(-1)^k}{(1+k)}\left(\begin{array}{l}\int_{\frac{\theta-1}{\omega_1}}^{\infty} f_g(x)\,e^{-\frac{(\theta-1)\lambda_{RD}}{\omega_2 x}}dx\\ -\int_{\frac{\theta-1}{\omega_1}}^{\infty} f_g(x)\,e^{-\frac{(\theta-1)\lambda_{RD}}{\omega_2 x}}e^{-\frac{(1+k)\omega_3\lambda_{RP}}{\omega_2 x}}dx\end{array}\right)\\
&= MN^2L\lambda_{SR}\lambda_{SP}\lambda_{RE}\sum_{l=0}^{L-1}\frac{C_{L-1}^{l}(-1)^l}{(1+l)\lambda_{RE}+\theta\lambda_{RD}}\\
&\left\{\sum_{k=0}^{N-1}\frac{C_{N-1}^{k}(-1)^k}{(1+k)}\sum_{m=0}^{M-1}C_{M-1}^{m}(-1)^m\sum_{n=0}^{N-1}C_{N-1}^{n}(-1)^n\left(\begin{array}{l}\underbrace{\int_{\frac{\theta-1}{\omega_1}}^{\infty}\frac{e^{-\frac{(\theta-1)\lambda_{RD}}{\omega_2 x}}}{\left[(1+n)\lambda_{SP}+(1+m)\lambda_{SR}x\right]^2}dx}_{I_1}\\ -\underbrace{\int_{\frac{\theta-1}{\omega_1}}^{\infty}\frac{e^{-\left[\frac{(\theta-1)\lambda_{RD}}{\omega_2}+\frac{(1+k)\omega_3\lambda_{RP}}{\omega_2}\right]\frac{1}{x}}}{\left[(1+n)\lambda_{SP}+(1+m)\lambda_{SR}x\right]^2}dx}_{I_2}\end{array}\right)\right\}
\end{aligned} \tag{19}$$

Lemma 4.1. *The following expression is valid for the integral* I_1.

$$\begin{aligned}
I_1 &= \int_{\frac{\theta-1}{\omega_1}}^{\infty}\frac{e^{-\frac{(\theta-1)\lambda_{RD}}{\omega_2 x}}}{\left[(1+n)\lambda_{SP}+(1+m)\lambda_{SR}x\right]^2}dx\\
&= \Phi\left(\frac{\omega_1}{\theta-1},(1+n)\lambda_{SP},(1+m)\lambda_{SR},\frac{(\theta-1)\lambda_{RD}}{\omega_2}\right)
\end{aligned}, \tag{20}$$

where $\Phi(u,a,b,p) \triangleq \frac{pe^{pb/a}}{a^2}\left[\Gamma\left(-1,\frac{pb}{a}\right)-\Gamma\left(-1,pu+\frac{pb}{a}\right)\right]$

Proof. Given in **Appendix B**. □

Similarly, we can obtain the following.

$$\begin{aligned}
I_2 &= \int_{\frac{\theta-1}{\omega_1}}^{\infty}\frac{e^{-\left[\frac{(\theta-1)\lambda_{RD}}{\omega_2}+\frac{(1+k)\omega_3\lambda_{RP}}{\omega_2}\right]\frac{1}{x}}}{\left[(1+n)\lambda_{SP}+(1+m)\lambda_{SR}x\right]^2}dx\\
&= \Phi\left(\frac{\omega_1}{\theta-1},(1+n)\lambda_{SP},(1+m)\lambda_{SR},\frac{(\theta-1)\lambda_{RD}}{\omega_2}+\frac{(1+k)\omega_3\lambda_{RP}}{\omega_2}\right)
\end{aligned} \tag{21}$$

Next, the term Pr 2 can be expressed as follows, including substitutions the PDFs of g, g_1, g_2 and g_3 into Eq. (15) and subsequent arrangements, similar to those used to obtain an expression for Pr 1.

$$\begin{aligned}
\Pr 2 &= \int_{\frac{\theta-1}{\omega_1}}^{\infty} f_g(x)\int_{\frac{\omega_3}{\omega_2 x}}^{\infty} f_{g_1}(x_1)\int_0^{\infty} f_{g_2}(x_2)\\
&\int_{\frac{\theta-1}{\omega_3}x_1+\theta x_2}^{\infty} f_{g_3}(x_3)dx_3dx_2dx_1dx\\
&= MN^2L\lambda_{SR}\lambda_{SP}\lambda_{RE}\lambda_{RP}\sum_{l=0}^{L-1}\frac{C_{L-1}^{l}(-1)^l}{(1+l)\lambda_{RE}+\theta\lambda_{RD}}\\
&\left\{\sum_{k=0}^{N-1}\frac{C_{N-1}^{k}(-1)^k}{(1+k)\lambda_{RP}+\frac{(\theta-1)\lambda_{RD}}{\omega_3}}\sum_{m=0}^{M-1}C_{M-1}^{m}(-1)^m\sum_{n=0}^{N-1}C_{N-1}^{n}(-1)^n\underbrace{\int_{\frac{\theta-1}{\omega_1}}^{\infty}\frac{e^{-\left[(1+k)\lambda_{RP}+\frac{(\theta-1)\lambda_{RD}}{\omega_3}\right]\frac{\omega_3}{\omega_2 x}}}{\left[(1+n)\lambda_{SP}+(1+m)\lambda_{SR}x\right]^2}dx}_{I_3}\right\}
\end{aligned} \tag{22}$$

The integral I_3 in Eq. (22) can be expressed as follows.

$$\begin{aligned}
I_3 &= \int_{\frac{\theta-1}{\omega_1}}^{\infty}\frac{e^{-\left[(1+k)\lambda_{RP}+\frac{(\theta-1)\lambda_{RD}}{\omega_3}\right]\frac{\omega_3}{\omega_2 x}}}{\left[(1+n)\lambda_{SP}+(1+m)\lambda_{SR}x\right]^2}dx\\
&= \Phi\left(\frac{\omega_1}{\theta-1},(1+n)\lambda_{SP},(1+m)\lambda_{SR},\left[(1+k)\lambda_{RP}+\frac{(\theta-1)\lambda_{RD}}{\omega_3}\right]\frac{\omega_3}{\omega_2}\right)
\end{aligned} \tag{23}$$

The secrecy outage probability of the system under the relay selection scheme MaSR can be obtained by combining Eqs. (13) and (19)âĂŞ(23) as follows.

$$\begin{aligned}
P_{out} &= 1 - MN^2L\lambda_{SR}\lambda_{SP}\lambda_{RE}\sum_{l=0}^{L-1}\frac{C_{L-1}^{l}(-1)^l}{(1+l)\lambda_{RE}+\theta\lambda_{RD}}\\
&\left\{\begin{array}{l}\left[\begin{array}{l}\sum_{k=0}^{N-1}\frac{C_{N-1}^{k}(-1)^k}{(1+k)}\sum_{m=0}^{M-1}C_{M-1}^{m}(-1)^m\sum_{n=0}^{N-1}C_{N-1}^{n}(-1)^n\\ \left(\begin{array}{l}\Phi\left(\frac{\omega_1}{\theta-1},(1+n)\lambda_{SP},(1+m)\lambda_{SR},\frac{(\theta-1)\lambda_{RD}}{\omega_2}\right)\\ -\Phi\left(\frac{\omega_1}{\theta-1},(1+n)\lambda_{SP},(1+m)\lambda_{SR},\right.\\ \left.\frac{(\theta-1)\lambda_{RD}}{\omega_2}+\frac{(1+k)\omega_3\lambda_{RP}}{\omega_2}\right)\end{array}\right]\\ +\lambda_{RP}\left[\begin{array}{l}\sum_{k=0}^{N-1}\frac{C_{N-1}^{k}(-1)^k}{(1+k)\lambda_{RP}+\frac{(\theta-1)\lambda_{RD}}{\omega_3}}\\ \sum_{m=0}^{M-1}C_{M-1}^{m}(-1)^m\sum_{n=0}^{N-1}C_{N-1}^{n}(-1)^n\\ \Phi\left(\frac{\omega_1}{\theta-1},(1+n)\lambda_{SP},(1+m)\lambda_{SR},\right.\\ \left.\left[(1+k)\lambda_{RP}+\frac{(\theta-1)\lambda_{RD}}{\omega_3}\right]\frac{\omega_3}{\omega_2}\right)\end{array}\right]\end{array}\right\}
\end{aligned} \tag{24}$$

4.2. Secrecy outage probability of MiRP

Under the MiRP relay selection scheme, the PDFs of the RVs g_1 and g are different from those given in Section 4.1. They are expressed as follows, including reference to proofs in **Appendix C** (Eq. C2) and **Appendix A** (Eq. A6), respectively

$$f_{g_1}(x_1) = MN\lambda_{RP}\sum_{u=0}^{N-1}C_{N-1}^{u}(-1)^{u}\sum_{m=0}^{M-1}C_{M-1}^{m}(-1)^{m}\sum_{k=0}^{Nm}C_{Nm}^{k}(-1)^{k}e^{-(1+u+k)\lambda_{RP}x_1} \tag{25}$$

$$f_{g}(x) = N\lambda_{SP}\lambda_{SR}\sum_{n=0}^{N-1}\frac{C_{N-1}^{n}(-1)^{n}}{\left[(1+n)\lambda_{SP}+\lambda_{SR}x\right]^{2}} \tag{26}$$

And the PDF of g_2 and g_3 are expressed as same as Section 4.1.

By the same way shown in Section 4.1, substituting the PDFs of 4 RVs g, g_1, g_2, and g_3 into (14) and (15), the terms Pr 1 and Pr 2 can be derived after some manipulations as follows.

$$\Pr 1 = MN^2L\lambda_{SR}\lambda_{SP}\lambda_{RE}\sum_{l=0}^{L-1}\frac{C_{L-1}^{l}(-1)^{l}}{(1+l)\lambda_{RE}+\theta\lambda_{RD}}\left\{\begin{array}{l}\sum_{u=0}^{N-1}C_{N-1}^{u}(-1)^{u}\sum_{m=0}^{M-1}C_{M-1}^{m}(-1)^{m}\\ \sum_{k=0}^{Nm}\frac{C_{Nm}^{k}(-1)^{k}}{1+u+k}\sum_{n=0}^{N-1}C_{N-1}^{n}(-1)^{n}\\ \left[\begin{array}{l}\Phi\left(\frac{\omega_1}{\theta-1},(1+n)\lambda_{SP},\lambda_{SR},\frac{(\theta-1)\lambda_{RD}}{\omega_2}\right)\\ -\Phi\left(\frac{\omega_1}{\theta-1},(1+n)\lambda_{SP},\lambda_{SR},\right.\\ \left.\frac{(\theta-1)\lambda_{RD}}{\omega_2}+\frac{(1+u+k)\omega_3\lambda_{RP}}{\omega_2}\right)\end{array}\right]\end{array}\right\} \tag{27}$$

$$\Pr 2 = MN^2L\lambda_{SR}\lambda_{SP}\lambda_{RE}\lambda_{RP}\sum_{l=0}^{L-1}\frac{C_{L-1}^{l}(-1)^{l}}{(1+l)\lambda_{RE}+\theta\lambda_{RD}} = \left\{\begin{array}{l}\sum_{u=0}^{N-1}C_{N-1}^{u}(-1)^{u}\sum_{m=0}^{M-1}C_{M-1}^{m}(-1)^{m}\\ \sum_{k=0}^{Nm}\frac{C_{Nm}^{k}(-1)^{k}}{(1+u+k)\lambda_{RP}+\frac{(\theta-1)\lambda_{RD}}{\omega_3}}\sum_{n=0}^{N-1}C_{N-1}^{n}(-1)^{n}\\ \Phi\left(\frac{\omega_1}{\theta-1},(1+n)\lambda_{SP},\lambda_{SR},\right.\\ \left.\left[(1+u+k)\lambda_{RP}+\frac{(\theta-1)\lambda_{RD}}{\omega_3}\right]\frac{\omega_3}{\omega_2}\right)\end{array}\right\} \tag{28}$$

The secrecy outage probability of the system under relay selection scheme MiSP can be expressed as follows by substituting Eqs. (27) and (28) into Eq. (13).

$$P_{out} = 1 - MN^2L\lambda_{SR}\lambda_{SP}\lambda_{RE}\sum_{l=0}^{L-1}\frac{C_{L-1}^{l}(-1)^{l}}{(1+l)\lambda_{RE}+\theta\lambda_{RD}}\left\{\begin{array}{l}\left\{\begin{array}{l}\sum_{u=0}^{N-1}C_{N-1}^{u}(-1)^{u}\sum_{m=0}^{M-1}C_{M-1}^{m}(-1)^{m}\\ \sum_{k=0}^{Nm}\frac{C_{Nm}^{k}(-1)^{k}}{1+u+k}\sum_{n=0}^{N-1}C_{N-1}^{n}(-1)^{n}\\ \left[\begin{array}{l}\Phi\left(\frac{\omega_1}{\theta-1},(1+n)\lambda_{SP},\lambda_{SR},\frac{(\theta-1)\lambda_{RD}}{\omega_2}\right)\\ -\Phi\left(\frac{\omega_1}{\theta-1},(1+n)\lambda_{SP},\lambda_{SR},\right.\\ \left.\frac{(\theta-1)\lambda_{RD}}{\omega_2}+\frac{(1+u+k)\omega_3\lambda_{RP}}{\omega_2}\right)\end{array}\right]\end{array}\right\}\\ +\lambda_{RP}\left\{\begin{array}{l}\sum_{u=0}^{N-1}C_{N-1}^{u}(-1)^{u}\sum_{m=0}^{M-1}C_{M-1}^{m}(-1)^{m}\\ \sum_{k=0}^{Nm}\frac{C_{Nm}^{k}(-1)^{k}}{(1+u+k)\lambda_{RP}+\frac{(\theta-1)\lambda_{RD}}{\omega_3}}\sum_{n=0}^{N-1}C_{N-1}^{n}(-1)^{n}\\ \Phi\left(\frac{\omega_1}{\theta-1},(1+n)\lambda_{SP},\lambda_{SR},\right.\\ \left.\left[(1+u+k)\lambda_{RP}+\frac{(\theta-1)\lambda_{RD}}{\omega_3}\right]\frac{\omega_3}{\omega_2}\right)\end{array}\right\}\end{array}\right\} \tag{29}$$

4.3. Secrecy outage probability of MiRE

The PDFs of only RVs g_2 and g in this relay selection scheme are changed compared to that in section 4.1 which are expressed respectively by the proof in **Appendix C** (Eq. C3) and **Appendix A** (Eq. A6) as follows

$$f_{g_2}(x_2) = ML\lambda_{RE}\sum_{l=0}^{L-1}C_{L-1}^{l}(-1)^{l}\sum_{m=0}^{M-1}C_{M-1}^{m}(-1)^{m}\sum_{u=0}^{Lm}C_{Lm}^{u}(-1)^{u}e^{-(1+l+u)\lambda_{RE}x_2} \tag{30}$$

$$f_{g}(x) = N\lambda_{SP}\lambda_{SR}\sum_{n=0}^{N-1}\frac{C_{N-1}^{n}(-1)^{n}}{\left[(1+n)\lambda_{SP}+\lambda_{SR}x\right]^{2}} \tag{31}$$

Then, we can obtain the following expressions for Pr 1 and Pr 2 in this relay selection scheme as follows

$$\begin{aligned}\Pr 1 &= \int_{\frac{\theta-1}{\omega_1}}^{\infty}f_g(x)\int_{0}^{\frac{\omega_3}{\omega_2 x}}f_{g_1}(x_1)\int_{0}^{\infty}f_{g_2}(x_2)\int_{\frac{\theta-1}{\omega_2 x}+\theta x_2}^{\infty}f_{g_3}(x_3)dx_3dx_2dx_1dx\\ &= MN^2L\lambda_{SR}\lambda_{SP}\lambda_{RE}\sum_{l=0}^{L-1}C_{L-1}^{l}(-1)^{l}\sum_{m=0}^{M-1}C_{M-1}^{m}(-1)^{m}\sum_{u=0}^{Lm}\frac{C_{Lm}^{u}(-1)^{u}}{(1+l+u)\lambda_{RE}+\theta\lambda_{RD}}\\ &\left\{\begin{array}{l}\sum_{k=0}^{N-1}\frac{C_{N-1}^{k}(-1)^{k}}{1+k}\sum_{n=0}^{N-1}C_{N-1}^{n}(-1)^{n}\\ \left[\begin{array}{l}\Phi\left(\frac{\omega_1}{\theta-1},(1+n)\lambda_{SP},\lambda_{SR},\frac{(\theta-1)\lambda_{RD}}{\omega_2}\right)dx\\ -\Phi\left(\frac{\omega_1}{\theta-1},(1+n)\lambda_{SP},\lambda_{SR},\right.\\ \left.\frac{(\theta-1)\lambda_{RD}}{\omega_2}+\frac{(1+k)\omega_3\lambda_{RP}}{\omega_2}\right)\end{array}\right]\end{array}\right\}\end{aligned} \tag{32}$$

$$\Pr 2 = \int_{\frac{\theta-1}{\omega_1}}^{\infty} f_g(x) \int_{\frac{\omega_3}{\omega_2 x}}^{\infty} f_{g_1}(x_1) \int_0^{\infty} f_{g_2}(x_2) \int_{\frac{\theta-1}{\omega_3}x_1+\theta x_2}^{\infty} f_{g_3}(x_3) dx_3 dx_2 dx_1 dx$$
$$= MN^2 L \lambda_{SR}\lambda_{SP}\lambda_{RE}\lambda_{RP} \sum_{l=0}^{L-1} C_{L-1}^{l}(-1)^l \sum_{m=0}^{M-1} C_{M-1}^{m}(-1)^m \sum_{u=0}^{Lm} \frac{C_{Lm}^{u}(-1)^u}{(1+l+u)\lambda_{RE}+\theta\lambda_{RD}}$$
$$\left\{ \sum_{k=0}^{N-1} \frac{C_{N-1}^{k}(-1)^k}{(1+k)\lambda_{RP}+\frac{(\theta-1)\lambda_{RD}}{\omega_3}} \sum_{n=0}^{N-1} C_{N-1}^{n}(-1)^n \left\{ \Phi\left(\frac{\omega_1}{\theta-1}, (1+n)\lambda_{SP}, \lambda_{SR}, \left[(1+k)\lambda_{RP} + \frac{(\theta-1)\lambda_{RD}}{\omega_3}\right]\frac{\omega_3}{\omega_2}\right)\right\} \right\} \tag{33}$$

Finally, the secrecy outage probability for the MiRE relay selection scheme can be expressed as follows.

$$P_{out} = 1 - MN^2 L \lambda_{SR}\lambda_{SP}\lambda_{RE} \sum_{l=0}^{L-1} C_{L-1}^{l}(-1)^l \sum_{m=0}^{M-1} C_{M-1}^{m}(-1)^m \sum_{u=0}^{Lm} \frac{C_{Lm}^{u}(-1)^u}{(1+l+u)\lambda_{RE}+\theta\lambda_{RD}}$$
$$\left\{ \sum_{k=0}^{N-1} \frac{C_{N-1}^{k}(-1)^k}{1+k} \sum_{n=0}^{N-1} C_{N-1}^{n}(-1)^n \left[\Phi\left(\frac{\omega_1}{\theta-1}, (1+n)\lambda_{SP}, \lambda_{SR}, \frac{(\theta-1)\lambda_{RD}}{\omega_2}\right)dx - \Phi\left(\frac{\omega_1}{\theta-1}, (1+n)\lambda_{SP}, \lambda_{SR}, \frac{(\theta-1)\lambda_{RD}}{\omega_2} + \frac{(1+k)\omega_3\lambda_{RP}}{\omega_2}\right) \right] \right.$$
$$\left. + \lambda_{RP} \left\{ \sum_{k=0}^{N-1} \frac{C_{N-1}^{k}(-1)^k}{(1+k)\lambda_{RP}+\frac{(\theta-1)\lambda_{RD}}{\omega_3}} \sum_{n=0}^{N-1} C_{N-1}^{n}(-1)^n \left\{ \Phi\left(\frac{\omega_1}{\theta-1}, (1+n)\lambda_{SP}, \lambda_{SR}, \left[(1+k)\lambda_{RP} + \frac{(\theta-1)\lambda_{RD}}{\omega_3}\right]\frac{\omega_3}{\omega_2} \right)\right\} \right\} \right\} \tag{34}$$

5. System performance with high Q/N_0

To provide insight into how the system parameters impact the network performance, we derive the asymptotic secrecy outage probability in the high Q/N_0 of the considered system. At high Q/N_0 with respect to $\frac{\theta-1}{\omega_1} \to 0$. Then, the value of the integral I_1 in (B1) is increased and can be approximated as:

$$I_1 \approx \int_0^{\infty} \frac{e^{-\frac{(\theta-1)\lambda_{RD}}{\omega_2 x}}}{\left[(1+n)\lambda_{SP}+(1+m)\lambda_{SR}x\right]^2} dx = \int_{\infty}^{0} \frac{-e^{-\frac{(\theta-1)\lambda_{RD}}{\omega_2}v}}{\left[(1+n)\lambda_{SP}v+(1+m)\lambda_{SR}\right]^2} dv = \int_0^{\infty} \frac{e^{-\frac{(\theta-1)\lambda_{RD}}{\omega_2}v}}{\left[(1+n)\lambda_{SP}v+(1+m)\lambda_{SR}\right]^2} dv \tag{35}$$

By applying the [31, Eq. 3.462.15] with $n = 2$: $\int_0^{\infty} \frac{e^{-px}}{(au+b)^2} dx = \frac{pe^{pb/a}}{a^2}\Gamma\left(-1, \frac{pb}{a}\right)$ to (35), we have

$$I_1 = \frac{(\theta-1)\lambda_{RD}}{\omega_2} \frac{e^{\frac{(1+m)(\theta-1)\lambda_{RD}\lambda_{SR}}{(1+n)\lambda_{SP}\omega_2}}}{(1+n)^2(\lambda_{SP})^2} \Gamma\left(-1, \frac{(1+m)(\theta-1)\lambda_{RD}\lambda_{SR}}{(1+n)\lambda_{SP}\omega_2}\right) \tag{36}$$

Similarly, we obtain the results for I_2 and I_3 as follows

$$I_2 \approx \int_0^{\infty} \frac{e^{-\left[\frac{(\theta-1)\lambda_{RD}}{\omega_2} + \frac{(1+k)\omega_3\lambda_{RP}}{\omega_2}\right]\frac{1}{x}}}{\left[(1+n)\lambda_{SP}+(1+m)\lambda_{SR}x\right]^2} dx = \frac{\left[\frac{(\theta-1)\lambda_{RD}}{\omega_2} + \frac{(1+k)\omega_3\lambda_{RP}}{\omega_2}\right] e^{\left[\frac{(\theta-1)\lambda_{RD}}{\omega_2} + \frac{(1+k)\omega_3\lambda_{RP}}{\omega_2}\right]\frac{(1+m)\lambda_{SR}}{(1+n)\lambda_{SP}}}}{(1+n)^2(\lambda_{SP})^2} \Gamma\left(-1, \left[\frac{(\theta-1)\lambda_{RD}}{\omega_2} + \frac{(1+k)\omega_3\lambda_{RP}}{\omega_2}\right]\frac{(1+m)\lambda_{SR}}{(1+n)\lambda_{SP}}\right) \tag{37}$$

$$I_3 \approx \int_{\frac{\theta-1}{\omega_1}}^{\infty} \frac{e^{-\left[(1+k)\lambda_{RP}+\frac{(\theta-1)\lambda_{RD}}{\omega_3}\right]\frac{\omega_3}{\omega_2 x}}}{\left[(1+n)\lambda_{SP}+(1+m)\lambda_{SR}x\right]^2} dx = \frac{\left[(1+k)\lambda_{RP}+\frac{(\theta-1)\lambda_{RD}}{\omega_3}\right]\frac{\omega_3}{\omega_2} e^{\frac{\left[(1+k)\lambda_{RP}+\frac{(\theta-1)\lambda_{RD}}{\omega_3}\right]\frac{\omega_3}{\omega_2}(1+m)\lambda_{SR}}{(1+n)\lambda_{SP}}}}{(1+n)^2(\lambda_{SP})^2} \Gamma\left(-1, \frac{\left[(1+k)\lambda_{RP}+\frac{(\theta-1)\lambda_{RD}}{\omega_3}\right]\frac{\omega_3}{\omega_2}(1+m)\lambda_{SR}}{(1+n)\lambda_{SP}}\right) \tag{38}$$

We can see that when Q/N_0 is high, I_1, I_2 and I_3 increase because the term $\frac{pe^{pb/a}}{a^2}\Gamma\left(-1, \frac{pb}{a}\right)$ is larger than the term $\frac{pe^{pb/a}}{a^2}\left[\Gamma\left(-1, \frac{pb}{a}\right) - \Gamma\left(-1, pu + \frac{pb}{a}\right)\right]$ due to $\Gamma\left(-1, pu + \frac{pb}{a}\right) > 0$, lead to the secrecy outage probability decreases.

6. Numerical results

This section presents secrecy outage probability analyses of the three relay selection schemes considered for use in the underlay cognitive cooperative network under physical layer security, including both the analytical results and the results of Monte Carlo experiments each including 10^5 independent trials. The analyses considered a network in a two-dimensional plane, with the following coordinates for the source S, the destination D, the relay cluster, the primary user cluster, and the eavesdropper cluster: $(0,0)$, $(1,0)$, $(x_R,0)$, (x_P,y_P), and (x_E,y_E), respectively. Hence, we have the distances $d_{SD} = 1$, $d_{SR} = x_R$, $d_{SP} = \sqrt{(x_P)^2 + (y_P)^2}$, $d_{RD} = \sqrt{(1-x_R)^2}$, and $d_{RE} = \sqrt{(x_R - x_E)^2 + (y_E)^2}$. In all simulations, we assumed the path loss $\beta = 3$, noise $N_0 = 1$, and the parameter $\mu = 1$ [21].

Figure 2 shows secrecy outage probabilities of the three relay selection schemes studied versus the power splitting ratio $\rho \in (0.01, 0.99)$, including both Monte Carlo simulation results and theoretical curves for each of three values for the number of relay nodes: $M = 1$, 3, and 5. The exact expressions for the secrecy outage probabilities of the MaSR, MiRP, and MiRE schemes are given as Eqs. (24), (29), and (34), respectively. The simulated and theoretical results matched very closely, demonstrating the accuracy of our analysis. The three protocols all achieved the same performance in the case of $M = 1$ because no relay selection process is used when there is only one relay node in the system.

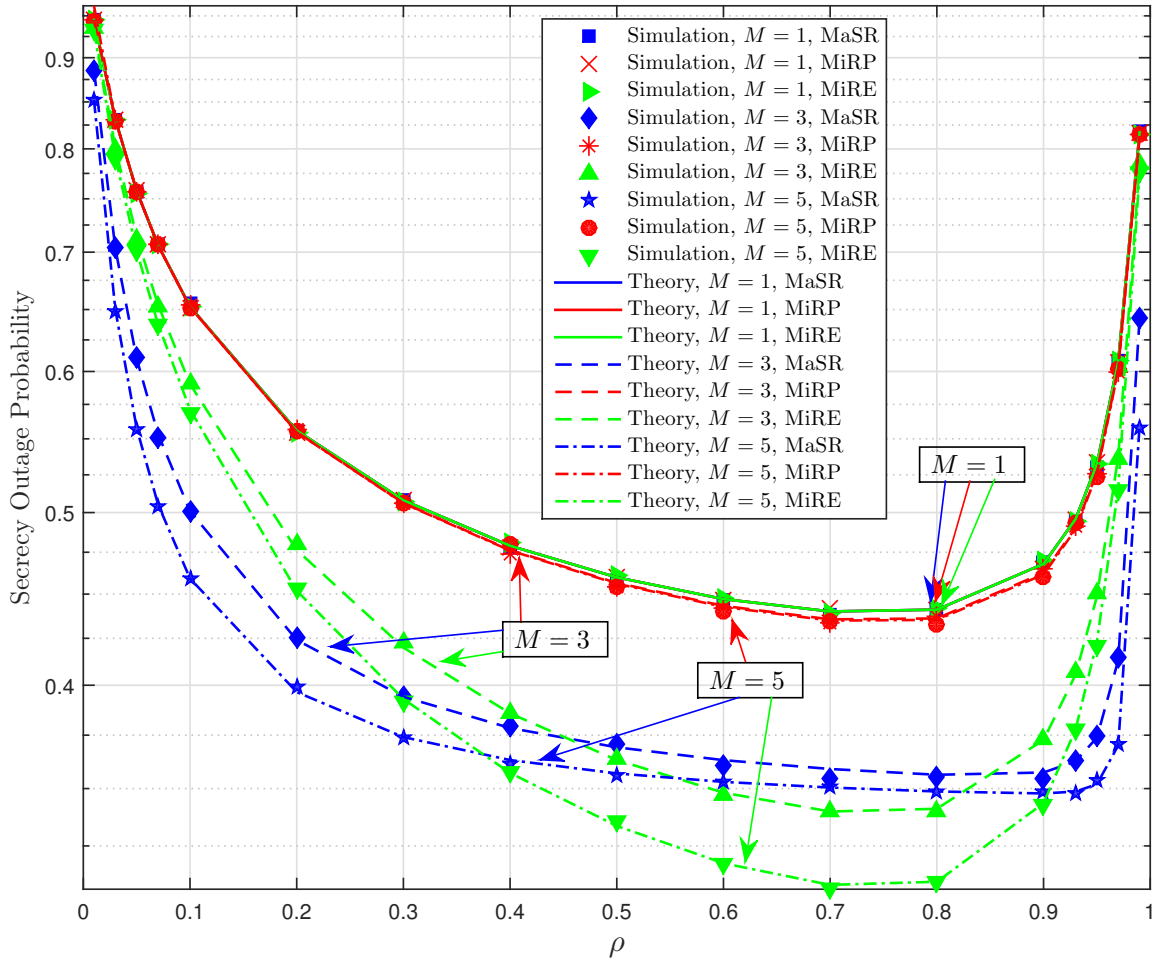

Figure 2. Secrecy outage probability versus the power splitting ratio ρ for the three protocols studied and for M of 1, 3, and 5, with $x_R = 0.5$, $(x_P, y_P) = (0.5, 1)$, $(x_E, y_E) = (0.8, -1)$, $Q = 10$ dB, $\eta = 0.9$, $\psi_t = 0.5$ bits/s/Hz, and $N = L = 2$.

The performance of all three protocols improved with increasing M; that is to say, the performance of each protocol was greater for $M = 5$ than for $M = 3$, and least for $M = 1$. These improvements can be explained as follows. As the number of relays is increased, the decoding quality and harvested energy at R_b is increased under MaSR, the effect upon R_b of power constraints from primary users is lessened under MiRP, and the impact of eavesdroppers is decreased under MiRE. However, the performance of the MiRP scheme improved very little with increasing M, and MiRP thus yielded the worst performance among the schemes for M greater than one. This occurred because in the presently considered scenario, the need for reducing the impact of power constraints from primary users is less than the needs for improving the decoding quality of the first hop (the $S - R$ link) and for diminishing the impact of eavesdroppers. In addition, the best performance was obtained for the case of MaSR with $\rho \approx 0.95$, and for the case of MiRP and MiRE with $\rho \approx 0.75$, demonstrating that these values of ρ are the optimal values for each protocol in this scenario. Finally, the MiRE scheme yielded the best performance among the three schemes when $\rho \in (0.4, 0.9)$.

Figure 3 illustrates the secrecy outage probability for the three relay selection schemes as a function of x_R, for various numbers of primary users N ($N = 1, 3, 5$). The outage performances of all three schemes worsened with increasing due to the increasing impact of power constraints imposed by the primary users upon the secondary network. The outage performance of the MaSR scheme was better than both the MiRP and MiRE schemes when the relay cluster is near the destination, i.e., $x_R \in (0.6, 0.9)$. The MiRE scheme attained better performance than the other two schemes when the relays were near the source ($x_R \in (0.1, 0.6)$). MiRP

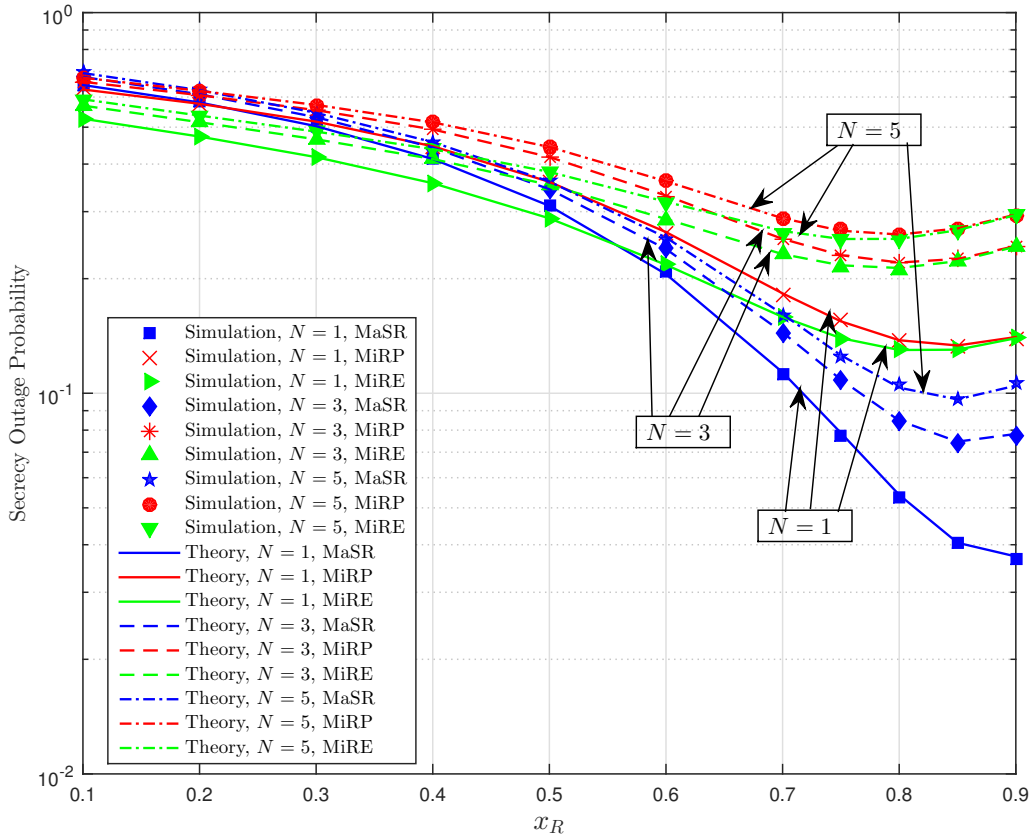

Figure 3. Secrecy outage probability versus x_R for the three protocols and for N of 1, 3, and 5, with $(x_P, y_P) = (0.5, 1)$, $(x_E, y_E) = (0.8, -1)$, $Q = 10$ dB, $\eta = 0.9$, $\rho = 0.5$, $\psi_t = 0.5$ bits/s/Hz, and $M = L = 2$.

performed the worst among the three schemes in this scenario.

Figure 4 shows the effect of the primary user cluster positions ($x_P = 0.5$, $y_P \in (0.1, 1)$) and the number of eavesdroppers $L = 1, 3, 5$ upon the outage performance of the three relay selection schemes. As expected, it can be seen that the outage probabilities of all three schemes increased with increasing L owing to the increasing impact of eavesdroppers upon the second hop. The outage performances of all three schemes were enhanced as the distance of primary users from the secondary network increased, thereby reducing the power constraints; that is to say, as y_P approached 1. The MaSR scheme performed better than both the MiRP and MiRE schemes in this scenario.

Figure 5 shows the effect of the eavesdropper position ($x_E = 0.8$, $y_E \in (-1, 0)$) upon the secrecy outage performance for three values of the secrecy target threshold. The outage performances of the three schemes worsened considerably as y_E approached 0, reaching a state of nearly full outage at $y_E = 0$. This phenomenon occurs because eavesdroppers closer to R_b and D can more easily overhear the information of the $R_b \to D$ link. Furthermore, the outage probability is also increased as the required target rate grows; that is to say, for $\psi_t = 0.7$, the outage probabilities of all three schemes are higher than those for $\psi_t = 0.5$ and for $\psi_t = 0.3$. In this scenario, the MiRE scheme performed better than both the MaSR and MiRP schemes.

Figure 6 shows the outage performances of the three schemes versus the interference threshold Q. The outage performance improved with increasing Q because of the greater allowed transmit power at the source and R_b. As expected, the outage performance also improves as the harvesting efficiency coefficient η increases, because the corresponds to increased harvested power at R_b. In this scenario, the MaSR yielded the best outage performance except for the case of $\eta = 0.9$ with Q over 8 dB.

7. Conclusions

We have proposed and analyzed an underlay cognitive cooperative energy harvesting relaying network under

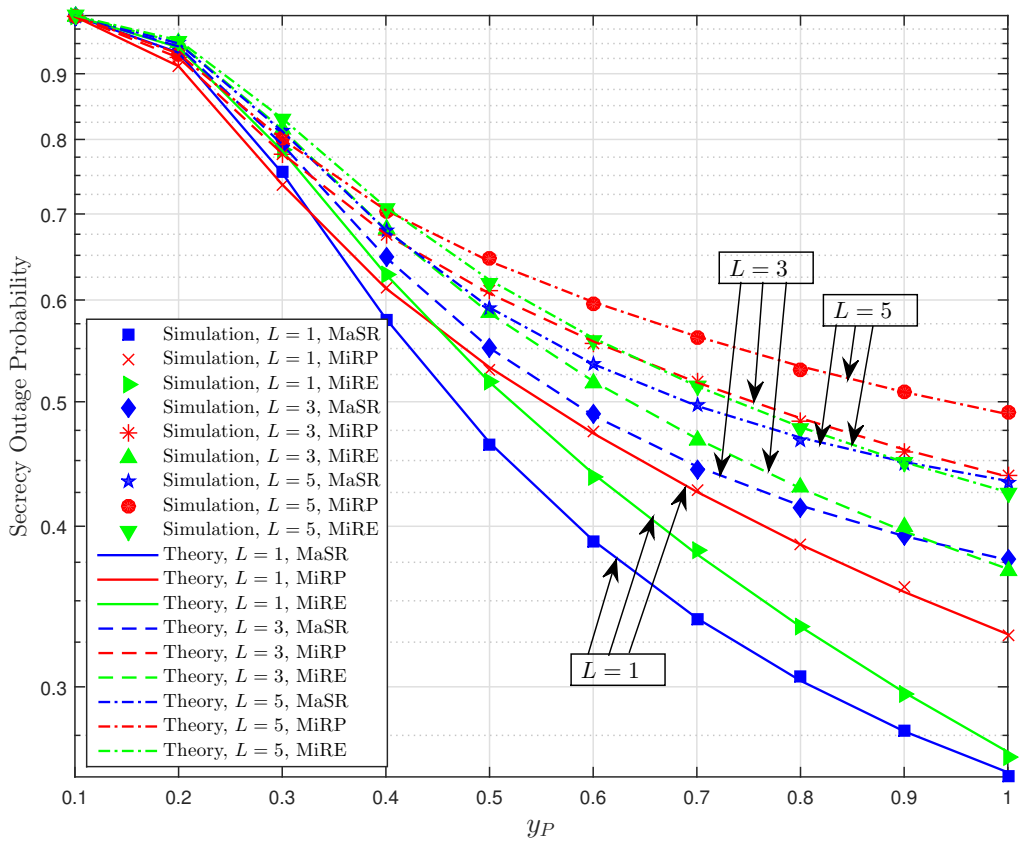

Figure 4. Secrecy outage probability versus y_P for the three protocols and for L of 1, 3, and 5, with $x_R = 0.5$, $x_P = 0.5$, $(x_E, y_E) = (0.8, -1)$, $Q = 10$ dB, $\eta = 0.9$, $\rho = 0.5$, $\psi_t = 0.5$ bits/s/Hz, and $M = N = 2$.

physical layer security. For comparison purposes, we presented three relay selection schemes for this model: MaSR, MiRP, and MiRE. Monte Carlo simulations were used to verify the theoretical expressions. The exact secrecy outage probability expressions agreed very well with the simulated curves in all scenarios. Through the simulation and theoretical results, it was discovered that 1) when either the number of relay nodes M is increased, the number of primary user nodes N is decreased, or the number of eavesdroppers L is decreased, the outage performances of all protocols are improved; 2) the outage performance of the system is enhanced when either the relays are located close to the destination, the primary users and the eavesdroppers are located far from the source, the required secrecy rate ψ_t is low, the energy harvesting efficiency η is high, or the interference threshold Q is high; 3) at the optimal power splitting ratio ρ, the secrecy outage probability of all three schemes are their lowest; 4) the MiRP scheme yields worse performance than the MaSR and MiRE schemes in all scenarios; and 5) the outage performance of the MaSR scheme is better than that of the MiRE scheme in almost all scenarios.

Appendix A: Finding the PDF of $g = \frac{g_{SR_b}}{\max\limits_{n=1,2,\ldots,N} g_{SP_n}} = \frac{g_4}{g_5}$, where $g_4 \triangleq g_{SR_b}$ and $g_5 \triangleq \max\limits_{n=1,2,\ldots,N} g_{SP_n}$, in three cases (three relay selections schemes)

Case 1. The MaSR relay selection scheme is applied: $R_b = \arg \max\limits_{m=1,2,\ldots,M} g_{SR_m}$ The CDF of RV is given by

$$F_{g_4}(x_4) = \Pr\left[g_{SR_b} < x_4\right] = \Pr\left[\max_{m=1,2,\ldots,M} g_{SR_m} < x_4\right] = \prod_{m=1}^{M} \Pr\left[g_{SR_m} < x_4\right] = \left(1 - e^{-\lambda_{SR} x_4}\right)^M \tag{A1}$$

The PDF for RV can be obtained by differentiating (A1) as

$$f_{g_4}(x_4) = M\lambda_{SR}\left(1 - e^{-\lambda_{SR} x_4}\right)^{M-1} = M\lambda_{SR} \sum_{m=0}^{M-1} C_{M-1}^{m} (-1)^m e^{-(1+m)\lambda_{SR} x_4} \tag{A2}$$

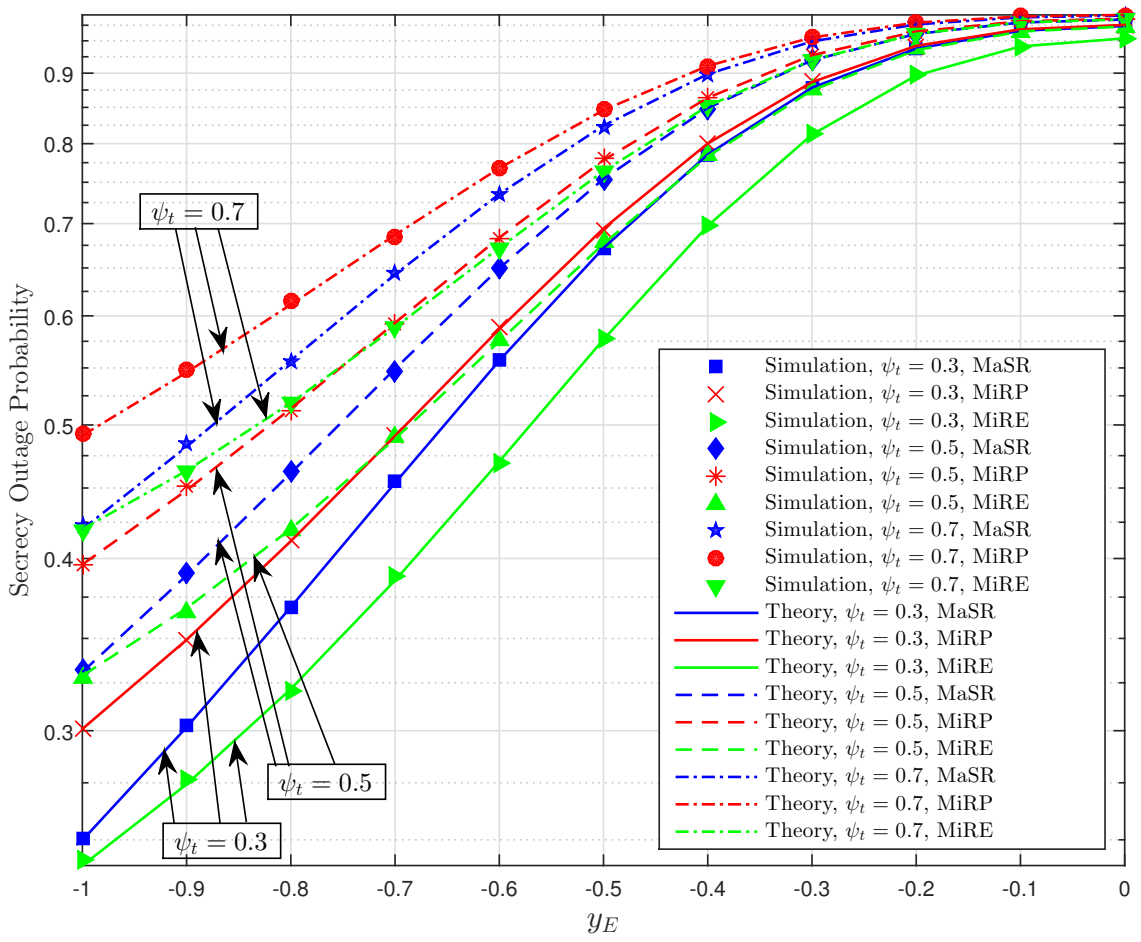

Figure 5. Outage probability of the PSX protocol with $\rho = 0.7$ (a) and TSX protocol with $\alpha = 0.9$ (b) versus η when $\psi = 10$ dB, $N = 3$, $x_R = 0.8$, $\psi_t = 1$.

Similarly, we also obtained

$$f_{g_5}(x_5) = N\lambda_{SP}\sum_{n=0}^{N-1} C_{N-1}^{n}(-1)^n e^{-(1+n)\lambda_{SP}x_5} \tag{A3}$$

The CDF of g can be expressed as follows, including using of Eqs. (A2) and (A3) and subsequent manipulations.

$$\begin{aligned} F_g(x) &= \Pr\left[\frac{g_4}{g_5} < x\right] \\ &= \int_0^{\infty} f_{g_5}(x_5)\int_0^{xx_5} f_{g_4}(x_4)dx_4dx_5 \\ &= M\sum_{m=0}^{M-1}\frac{C_{M-1}^{m}(-1)^m}{1+m}\left[1 - N\lambda_{SP}\sum_{n=0}^{N-1}\frac{C_{N-1}^{n}(-1)^n}{(1+n)\lambda_{SP}+(1+m)\lambda_{SR}x}\right] \end{aligned} \tag{A4}$$

By differentiating (A4), we obtain the PDF of g as follows

$$\begin{aligned} f_g(x) &= MN\lambda_{SP}\lambda_{SR} \\ &\sum_{m=0}^{M-1} C_{M-1}^{m}(-1)^m \sum_{n=0}^{N-1}\frac{C_{N-1}^{n}(-1)^n}{[(1+n)\lambda_{SP}+(1+m)\lambda_{SR}x]^2} \end{aligned} \tag{A5}$$

Case 2. The MiRP relay selection scheme is applied:

$$R_b = \arg\min_{m=1,2,\ldots,M}\left(\max_{n=1,2,\ldots,N} g_{R_mP_n}\right)$$

Case 3. The MiRE relay selection scheme is applied:

$$R_b = \arg\min_{m=1,2,\ldots,M}\left(\max_{l=1,2,\ldots,L} g_{R_mE_l}\right)$$ The PDFs of g_4 and g_5 in cases 2 and 3 are the same and given as follows $f_{g_4}(x_4) = \lambda_{SR}e^{-\lambda_{SR}x_4}$,

$$f_{g_5}(x_5) = N\lambda_{SP}\sum_{n=0}^{N-1} C_{N-1}^{n}(-1)^n e^{-(1+n)\lambda_{SP}x_5}.$$

After some manipulations as same as that in case 1, we can obtain the PDF for g in both cases 2 and 3 as follows

$$f_g(x) = N\lambda_{SP}\lambda_{SR}\sum_{n=0}^{N-1}\frac{C_{N-1}^{n}(-1)^n}{[(1+n)\lambda_{SP}+\lambda_{SR}x]^2} \tag{A6}$$

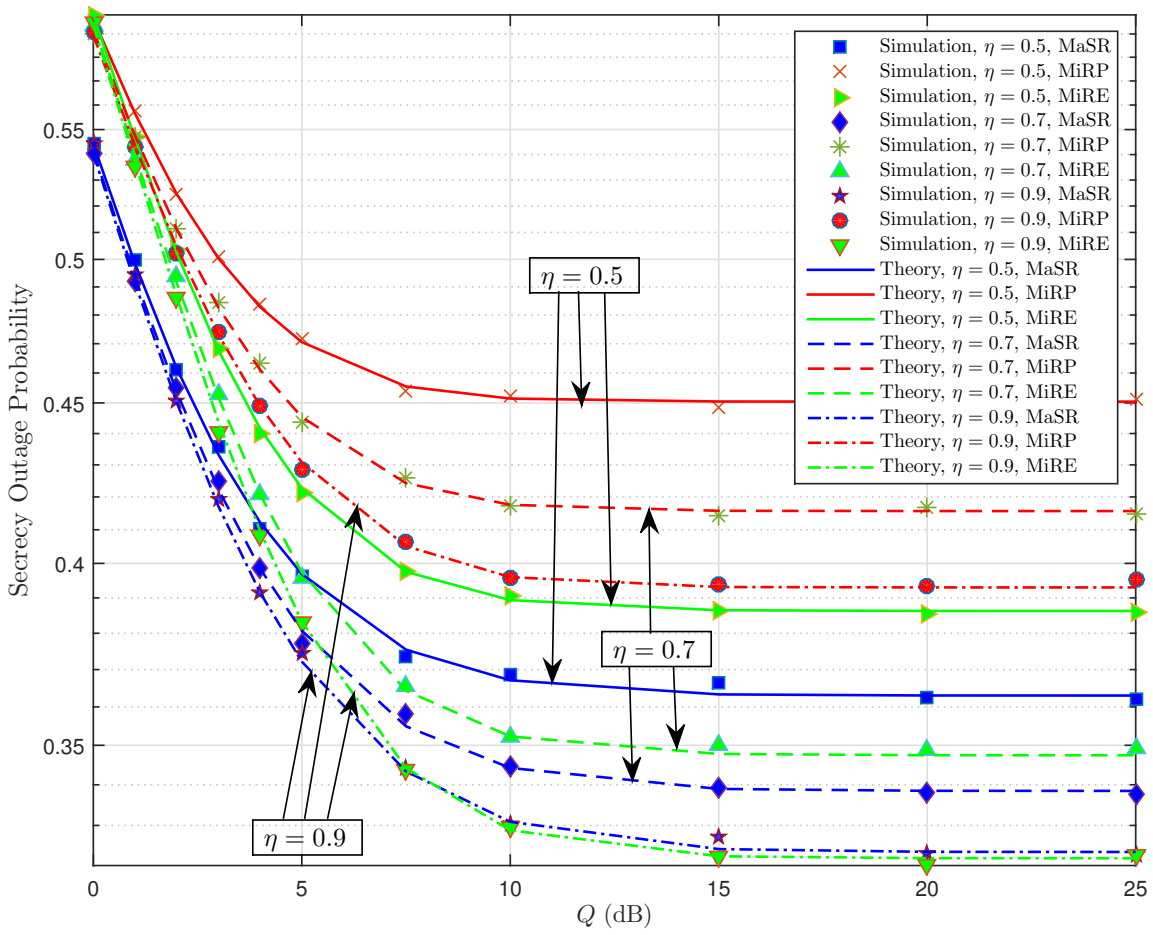

Figure 6. Throughput performance of PSX protocol with $\rho = 0.7$ and TSX protocol with $\alpha = 0.9$ versus the target SNR ψ_t when $\psi = 10$ dB, $N = 3$, $x_R = 0.8$, $\eta = 0.9$, $\mu = 1$.

Appendix B: Proof of Lemma 1

By setting $v = \frac{1}{x}$, we obtain $dx = -x^2$, $dv = -\frac{1}{v^2}dv$. The integral I_1 can be rewritten as

$$\begin{aligned} I_1 &= \int_{\frac{\theta-1}{\omega_1}}^{\infty} \frac{e^{-\frac{(\theta-1)\lambda_{RD}}{\omega_2 x}}}{\left[(1+n)\lambda_{SP}+(1+m)\lambda_{SR}x\right]^2}dx \\ &= \int_{\frac{\omega_1}{\theta-1}}^{0} \frac{-e^{-\frac{(\theta-1)\lambda_{RD}}{\omega_2}v}}{\left[(1+n)\lambda_{SP}v+(1+m)\lambda_{SR}\right]^2}dv \\ &= \int_{0}^{\frac{\omega_1}{\theta-1}} \frac{e^{-\frac{(\theta-1)\lambda_{RD}}{\omega_2}v}}{\left[(1+n)\lambda_{SP}v+(1+m)\lambda_{SR}\right]^2}dv \end{aligned} \tag{B1}$$

By using the [31, Eq. 3.462.17] with $n = 2$, we have

$$\begin{aligned} &\int_0^u \frac{e^{-px}}{(ax+b)^2}dx = \frac{pe^{pb/a}}{a^2}\left[\Gamma\left(-1, \frac{pb}{a}\right) - \Gamma\left(-1, pu + \frac{pb}{a}\right)\right] \\ &\triangleq \Phi\left(u, a, b, p\right) \end{aligned} \tag{B2}$$

By using (B2) into (B1), we obtain

$$\begin{aligned} I_1 &= \int_0^{\frac{\omega_1}{\theta-1}} \frac{e^{-\frac{(\theta-1)\lambda_{RD}}{\omega_2}u}}{\left[(1+n)\lambda_{SP}u+(1+m)\lambda_{SR}\right]^2}du \\ &= \Phi\left(\frac{\omega_1}{\theta-1}, (1+n)\lambda_{SP}, (1+m)\lambda_{SR}, \frac{(\theta-1)\lambda_{RD}}{\omega_2}\right) \end{aligned} \tag{B3}$$

Appendix C: Finding the PDF of $g_1 \triangleq \max\limits_{n=1,2,\ldots,N} g_{R_bP_n} = \min\limits_{m=1,2,\ldots,M}\left(\max\limits_{n=1,2,\ldots,N} g_{R_mP_n}\right)$ for the MiRP scheme and $g_2 \triangleq \max\limits_{l=1,2,\ldots,L} g_{R_bE_l} = \min\limits_{m=1,2,\ldots,M}\left(\max\limits_{l=1,2,\ldots,L} g_{R_mE_l}\right)$ for the MiRE scheme

First, we derive the expression for the CDF of g_1 for the

MiRP scheme as

$$\begin{aligned} F_{g_1}(x_1) &= \Pr\left[\min_{m=1,2,\ldots,M}\left(\max_{n=1,2,\ldots,N} g_{R_m P_n}\right) < x_1\right] \\ &= 1 - \prod_{m=1}^{M}\left\{1 - \prod_{n=1}^{N}\Pr\left[g_{R_m P_n} < x_1\right]\right\} \\ &= 1 - \left[1 - \left(1 - e^{-\lambda_{RP} x_1}\right)^N\right]^M \end{aligned} \tag{C1}$$

Next, by differentiating (C1), we obtain the PDF of g_1 for the MiRP scheme as follows

$$\begin{aligned} & f_{g_1}(x_1) = MN\lambda_{RP} e^{-\lambda_{RP} x}\left(1 - e^{-\lambda_{RP} x_1}\right)^{N-1} \\ & \left[1 - \left(1 - e^{-\lambda_{RP} x_1}\right)^N\right]^{M-1} \\ & = MN\lambda_{RP} \sum_{n=0}^{N-1} C_{N-1}^{n} (-1)^n \sum_{m=0}^{M-1} C_{M-1}^{m} (-1)^m \\ & \sum_{k=0}^{Nm} C_{Nm}^{u} (-1)^u e^{-(1+n+k)\lambda_{RP} x_1} \end{aligned} \tag{C2}$$

Similarly, we can obtain g_2 for the MiRE scheme:

$$\begin{aligned} & f_{g_2}(x_2) = ML\lambda_{RE} \sum_{l=0}^{L-1} C_{L-1}^{l} (-1)^l \sum_{m=0}^{M-1} C_{M-1}^{m} (-1)^m \\ & \sum_{u=0}^{Lm} C_{Lm}^{u} (-1)^u e^{-(1+l+u)\lambda_{RE} x_2} \end{aligned} \tag{C3}$$

References

[1] Varshney, L. R. (2008). Transporting information and energy simultaneously. In: IEEE International Symposium on Information Theory (ISIT 2008), pp 1612-1616

[2] Zhou, X., Zhang, R., & Ho, C. K. (2013). Wireless Information and Power Transfer: Architecture Design and Rate-Energy Tradeoff. IEEE Trans Commun 61(11):4754-4767

[3] Nosratinia, A., Hunter, T. E., & Hedayat, A. (2004). Cooperative communication in wireless networks, IEEE Commun Maga 42(10):74-80

[4] Laneman, J. N., Tse D. N. C., & Wornell, G. W. (2004). Cooperative diversity in wireless networks: Efficient protocols and outage behavior. IEEE Trans Inf Theory 50(12):3062-3080

[5] Alouane, W. H., Hamdi, N., & Meherzi, S. (2014). Semi-blind amplify-and-forward in two-way relaying networks. Ann Telecommun 69(9):497âĹŠ508

[6] Alouane, W. H., & Hamdi, N. (2015). Semi-blind two-way AF relaying over Nakagami-m fading environment. Ann Telecommun 70(1):49âĹŠ62

[7] Alouane, W. H., & Hamdi, N. (2015). Performance analysis of semi-blind two way AF relaying over generalized-k fading channels. Ann Telecommun 70(9):381âĹŠ394

[8] Touati, S., Boujemmaa, H., & Abed, N. (2015). Static hybrid multihop relaying and two hops hybrid relaying using DSTC. Ann Telecommun 70(3):171âĹŠ180

[9] Liu, Y., Wang, L., Elkashlan, M., Duong, T. Q., & Nallanathan, A. (2014). Two-way relaying networks with wireless power transfer: Policies design and throughput analysis. In: Proceedings of IEEE global telecommunications conference (GLOBECOM2014). Austin, TX, pp 4030-4035

[10] Nasir, A. A., Zhou, X., Durrani, S., & Kennedy, R. A. (2013). Relaying Protocols for Wireless Energy Harvesting and Information Processing. IEEE Trans Wirel Commun 12(7):3622-3636

[11] Ding, Z., Perlaza, S.M., Esnaola I., & Poor H. V. (2014). Power Allocation Strategies in Energy Harvesting Wireless Cooperative Networks. IEEE Trans Wirel Commun 13(2):846-860

[12] Chu, Z., Johnston, M., & Goff, S.L. (2015). SWIPT for wireless cooperative networks. Electron Lett 51(6):536-538

[13] Velkov, Z. H.-, Zlatanov, N., Duong, T. Q., & Schober, R. (2015). Rate Maximization of Decode-and-Forward Relaying Systems With RF Energy Harvesting. IEEE Commun Lett 19(2):2290-2293

[14] Li, T., Fan, P., & Letaief, K. B. (2016). Outage Probability of Energy Harvesting Relay-Aided Cooperative Networks Over Rayleigh Fading Channel. IEEE Trans Vehi Techno 65(2):972-978

[15] Ding, Z., Krikidis, L., Sharif, B., & Poor, H. V. (2014). Wireless Information and Power Transfer in Cooperative Networks With Spatially Random Relays. IEEE Trans Wirel Commun 13(8):4440-4453

[16] Akyildiz, L. F., Lee, W.- Y., Vuran, M. C., & Mohanty, S. (2008). A survey on spectrum management in cognitive radio networks. IEEE Commun Maga 46(4):40-48

[17] Duong, T. Q., Costa, D. Bd., Tsiftsis, T. A., Zhong, C., & Nallanathan, A. (2012). Outage and Diversity of Cognitive Relaying Systems under Spectrum Sharing Environments in Nakagami-m Fading. IEEE Commun Lett 16(12):2075-2078

[18] Bao, V. N. Q., Duong, T. Q., Costa, D. Bd., Alexandropoulos, G. C., & Nallanathan, A. (2013). Cognitive Amplify-and-Forward Relaying with Best Relay Selection in Non-Identical Rayleigh Fading. IEEE Commun Lett 17(3):475-478

[19] Lu, X., Xu, W., Li, S., Lin, J., & He, Z. (2014). Simultaneous information and power transfer for relay-assisted cognitive radio networks. In: Proceedings of IEEE international communications (ICC 14). pp 331-336

[20] Yang, Z., Ding, Z., Fan, P., & Karagiannidis, G. (2015). Outage Performance of Cognitive Relay Networks with Wireless Information and Power Transfer. IEEE Trans Vehi Techno PP(99):1-6, doi: 10.1109/TVT.2015.2443875

[21] Son, P. N, & Kong, H. Y. (2015). Exact Outage Analysis of Energy Harvesting Underlay Cooperative Cognitive Networks. IEICE Trans Commun E98-B(4):661-672

[22] Nguyen, D. K., Matthaiou, M., Duong, T. Q., & Ochi, H. (2015). RF energy harvesting two-way cognitive DF relaying with transceiver impairments. In: Proceedings of IEEE international communications (ICC 15), London, UK, pp 1970-1975

[23] Wyner, A. D. (1975). The wire-tap channel. The Bell Syst Techni Journal 54(8):1355-1387 63(8):1993–2006

[24] Cheong, S. L.- Y.-, & Hellman, M. (1978). The Gaussian wire-tap channel. IEEE Trans Inf Theory 24(4):451-456

[25] Csiszar, I., & Korner, J. (1978). Broadcast channels with confidential messages. IEEE Trans Inf Theory 24(3):339-348

[26] Liang, Y., Poor, H. V., & Shamai, S. (2008). Secure Communication Over Fading Channels. IEEE Trans Inf Theory 54(6):2470-2492

[27] Elkashlan, M., Wang, L., Duong, T. Q., Karagiannidis, G. K., & Nallanathan, A. (2015). On the Security of Cognitive Radio Networks. IEEE Trans Vehi Techno 64(8):3790-3795

[28] Liu, Y., Wang, L., Duy, T. T., Elkashlan, M., & Duong, T. Q. (2015). Relay Selection for Security Enhancement in Cognitive Relay Networks. IEEE Wirel Commun Lett 4(1):46-49

[29] Fan, L., Zhang, S., Duong, T. Q., & Karagiannidis, G. K. (2016). Secure Switch-and-Stay Combining (SSSC) for Cognitive Relay Networks. IEEE Trans Commun 64(1):70-82

[30] Son, P. N., & Kong, H. Y. (2015). Cooperative communication with energy-harvesting relays under physical layer security. IET Commun 9(17):2131-2139

[31] Gradshteyn, I. S, & Ryzhik, I. M. (2007). Table of integrals, series and products. 7th ed. Academic Press

[32] Yeoh, P. L., Yang, N., Kim, K. J. (2015). Secrecy Outage Probability of Selective Relaying Wiretap Channels with Collaborative Eavesdropping. In: Proceedings of IEEE global telecommunications conference (GLOBECOM2015), San Diego, CA, USA, pp 1-6